above, and the cochleae were collected 7 days after surgery. The remaining four animals were preserved as controls, receiving no surgical treatment.

Immunohistochemistry

Under general anesthesia with ketamine and xylazine, animals were perfused intracardially with ice-cooled phosphate-buffered saline (PBS), followed by 4% paraformaldehyde in phosphate buffer. The temporal bones were collected and immersed in the same fixative for 4 hr at 4°C. The samples were decalcified with 10% EDTA in PBS and cryoprotected with 30% sucrose. Specimens were prepared as cryostat sections (10 μm in thickness). Midmodiolar sections were provided for histological analyses.

Cryostat sections were immersed in blocking solution containing 10% goat serum for 30 min and incubated with a primary antibody at 4°C overnight. Characteristics of BM-derived cells were examined by immunostaining for leukocyte common antigen CD45; ionized calcium binding adapter molecule 1 (Iba1), which is specific for microglia/macrophages (Imai et al., 1996); microglia/macrophage-specific glycoprotein F4/80; and macrosialin CD68, which is specifically expressed by tissue macrophages. Immunohistochemistry for Ki67, a nuclear protein expressed in proliferating cells, was performed on the BM chimeric mice to determine the proliferation of BM-derived cells in situ. The primary antibodies used in this study were rat anti-mouse CD45 (1:50; 30-F11; BD Pharmingen), rabbit anti-Iba1 (1:1,000; Wako Pure Chemicals, Osaka, Japan), rat anti-mouse F4/80 (1:10; Cl:A3-1; Serotec, Oxford, United Kingdom), rat anti-mouse CD68 (1:1,000; FA-11; Serotec), and rabbit anti-Ki67 (1:200; SP6; Lab Vision, Fremont, CA). The localization of primary antibodies was visualized using secondary antibodies conjugated with Alexa Fluor 488, 555, or 633 (1:500; Molecular Probes, Eugene, OR). Nuclei were counterstained by 4′,6-diamidino,2-phenylindole dihydrochloride (DAPI; 1 mg/ml in PBS; Molecular Probes). Negative controls lacked primary antibody labeling. Specimens were viewed with a Nikon Eclipse E600 fluorescence microscope (Nikon, Tokyo, Japan) or a Leica TCS-SP2 confocal laser scanning microscope (Leica Microsystems, Tokyo, Japan) with a digital image-capture system.

Quantification

To determine the chimeric ratio in peripheral blood, smears of blood samples were made on slides. Total cells with nuclei were based on nuclear counts with DAPI staining observed with a fluorescence microscope. The ratio of EGFP-positive cells to the total number of cells was calculated. At least 200 nuclei were counted in each sample.

For the quantitatification of BM-derived cells or Iba1-positive cells, four sections were selected randomly from the 12 most midmodiolar sections for each experimental or control animal. To assess the distribution of BM-derived cells in the cochlea, the number of cells derived from engrafted HSCs in one midmodiolar section from base to apex was counted in six animals at 6 months after HSC transplantation. All BM-derived cells defined by coexpression of EGFP and DAPI within the cochlea were counted by two double-blinded examiners. The number of HSC-derived cells coexpressing Iba1, F4/80, CD45, or CD68 was also counted for examination of the phenotype of BM-derived cells. The ratio of EGFP-positive cells labeled with Iba1, F4/80, CD45, or CD68 to the total number of EGFP-positive cells was calculated. To study the replacement of Iba1-positive cells in the cochlea by engrafted EGFP-positive cells, the number of cells dual-labeled with EGFP and Iba1 in one midmodiolar section was counted. The ratio of the expression of EGFP to the total number of Iba1-positive cells was calculated in the cochleae harvested at 1, 2, or 4 weeks and 3, or 6 months after HSC transplantation. To investigate the dynamics of EGFP- or Iba1-positive cells in the cochlea, the density of EGFP- or Iba1-positive cells in SG was calculated by a modified method as described previously for evaluating the density of SG neurons (Shinohara et al., 2002). All EGFP- or Iba1-positive cells with nuclei stained for DAPI within each profile of Rosenthal's canal from the midbasal portion of the cochlea were counted. The outline of Rosenthal's canal profile was then traced under a brightfield image to generate the area of SG in Image J software (http://www.nist.gov/lispix/imlab/prelim/dnld.html). The density of EGFP- or Iba1-positive cells in SG was expressed as the cell number for an area of 10,000 μm^2. The density of EGFP- or Iba1-positive cells in SL of midbasal portion of the cochlea was also calculated by tracing the outline of the SL region occupied by type I-V fibrocytes and expressed as the cell number for an area of 10,000 μm^2. The number of total cells in the area of interest was determined by counting nuclei on DAPI-stained sections in Image J software. The number of proliferating macrophages in the cochlea was determined by counting the colocalization of Ki67 and DAPI. The ratio of EGFP-positive cells labeled with Ki67 to the total number of CD68-positive cells per section was also calculated.

Statistcal Analysis

Statistical analyses were performed by using one-way analysis of variance (ANOVA) followed by the Tukey-Kramer's test, for the analysis of ABR thresholds, alteration of Iba1-positive cells by EGFP-positive cells, and effect of local surgical stress. An unpaired *t*-test was used in other statistical analyses. $P < 0.05$ was considered statistically significant. All data are presented as the mean ± SE.

RESULTS

BM-Derived Cells Are Widely Distributed in the Spiral Ganglion and the Spiral Ligament

Six months after BM transplantation, numerous EGFP-positive cells were found widely within the cochlea of transplanted mice (Fig. 1a). A large population of EGFP-positive cells is located in the connective tissue of SL and auditory nervous system, including SG and acoustic nerve (AN; Fig. 1b–d). In SL, EGFP-positive cells were observed predominantly in its lower portion, corresponding to the type II and IV fibrocyte regions (Fig. 1b). In the auditory nervous system, EGFP-positive cells were observed along nerve fibers both in SG and

F1

COLOR

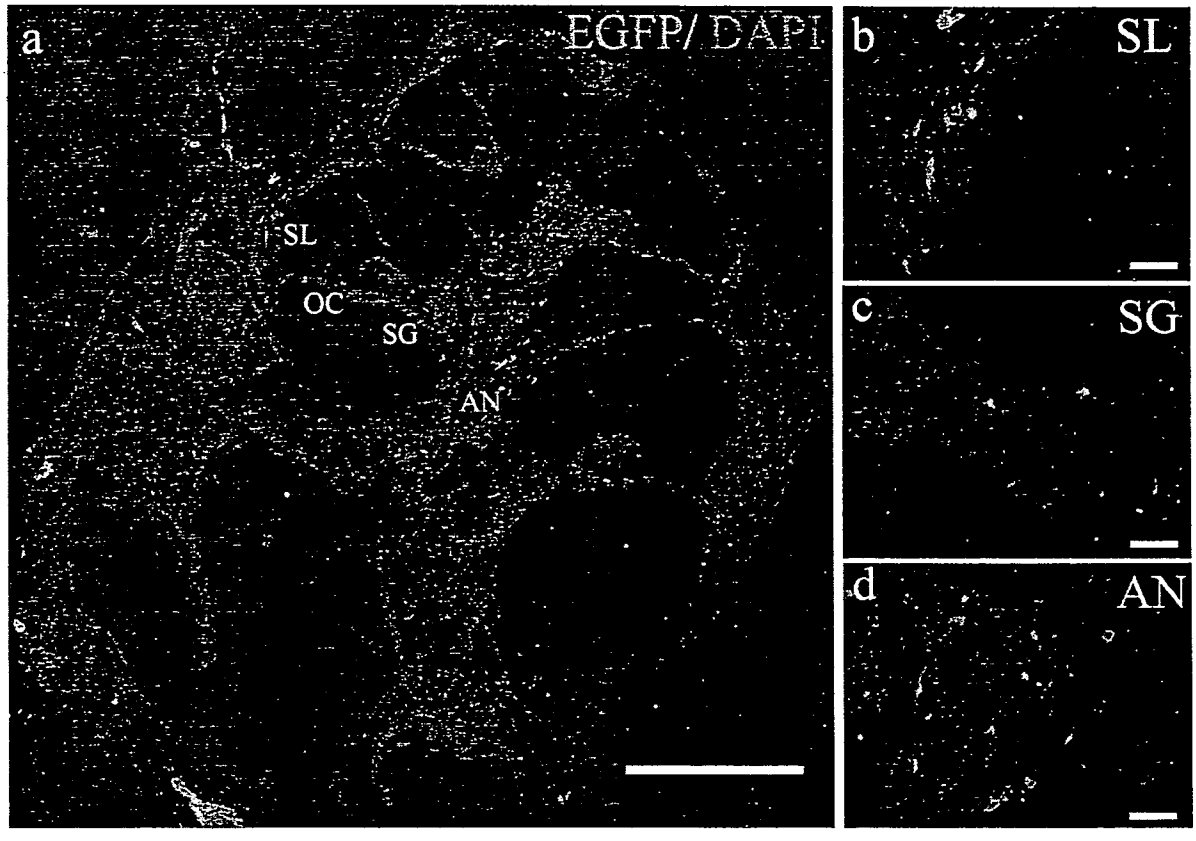

Fig. 1. Distribution of hematopoietic cell-derived cells in the cochlea. **a:** Distribution of hematopoietic cell-derived cells is shown in a midmodiolar section obtained from bone marrow (BM) chimeric mice 6 months after transplantation. BM-derived cells expressing EGFP were distributed from the base to the apex of the cochlea. Blue fluorescence shows nuclear staining with DAPI. **b–d:** In SL, EGFP-positive cells were observed predominantly in the lower portion of SL occupied by type II and IV fibrocytes (b). In the auditory nervous system, EGFP-positive cells were observed along nerve fibers in both SG (c) and cochlear modiolus (d). AN, auditory nerve; OC, organ of Corti; SG, spiral ganglion; SL, spiral ligament. Scale bars = 500 μm in a; 50 μm in b–d.

AN (Fig. 1c,d). In one midmodiolar section obtained at 6 months after transplantation, 90.3 ± 6.9 cells expressing EGFP were observed, 35.6% ± 3.1% of which were in the cochlear connective tissues of SL and the spiral limbus and 62.2% ± 3.0% in the cochlear nervous system, including SG and AN. The proportion of BM-derived cells to the total cells was 7.7% ± 0.9% in SL and 5.5% ± 0.9% in SG, which was compatible with the study by Lang et al. (2006). EGFP-positive cells were occasionally identified on the undersurface of the basilar membrane in the scala tympani and in the stria vascularis (data not shown). No EGFP-positive cells were observed within the cochlear sensory epithelium.

More Than 80% of BM-Derived Cells in the Cochlea Demonstrated the Phenotype of Macrophages

The following analyses of immunohistochemistry were carried out to characterize hematopoietic BM-derived cells in the adult mouse cochlea. Most EGFP-positive cells expressed F4/80 (Fig. 2a), Iba1 (Fig. 2b), or CD68 (Fig. 2c), indicating that cochlear HSC-derived cells have differentiated into the macrophage lineage. Cells dually labeled with EGFP and Iba1, EGFP, or F4/80 or with EGFP and CD68 were localized both in the cochlear connective tissue and the cochlear nervous system. The expression of Iba1 was found in 92.5% ± 3.1% of EGFP-positive cells, and F4/80 expression was observed in 87.3% ± 4.2%. Although more than 80% of BM-derived cells in the cochlea demonstrated the phenotype of macrophage, immunoreactivity for CD45, a common leukocyte antigen, was identified in only 7.4% ± 0.5% of EGFP-positive cells in the cochlea of BM chimeric mice. The number of cells doubly stained with Iba1 and CD45 was limited to one or two in one section (0.9% ± 0.3% of the total number of Iba1-positive BM-derived cells) except for cells in BM of the temporal bone. In contrast, CD68 expression was found in 81.7%

F2

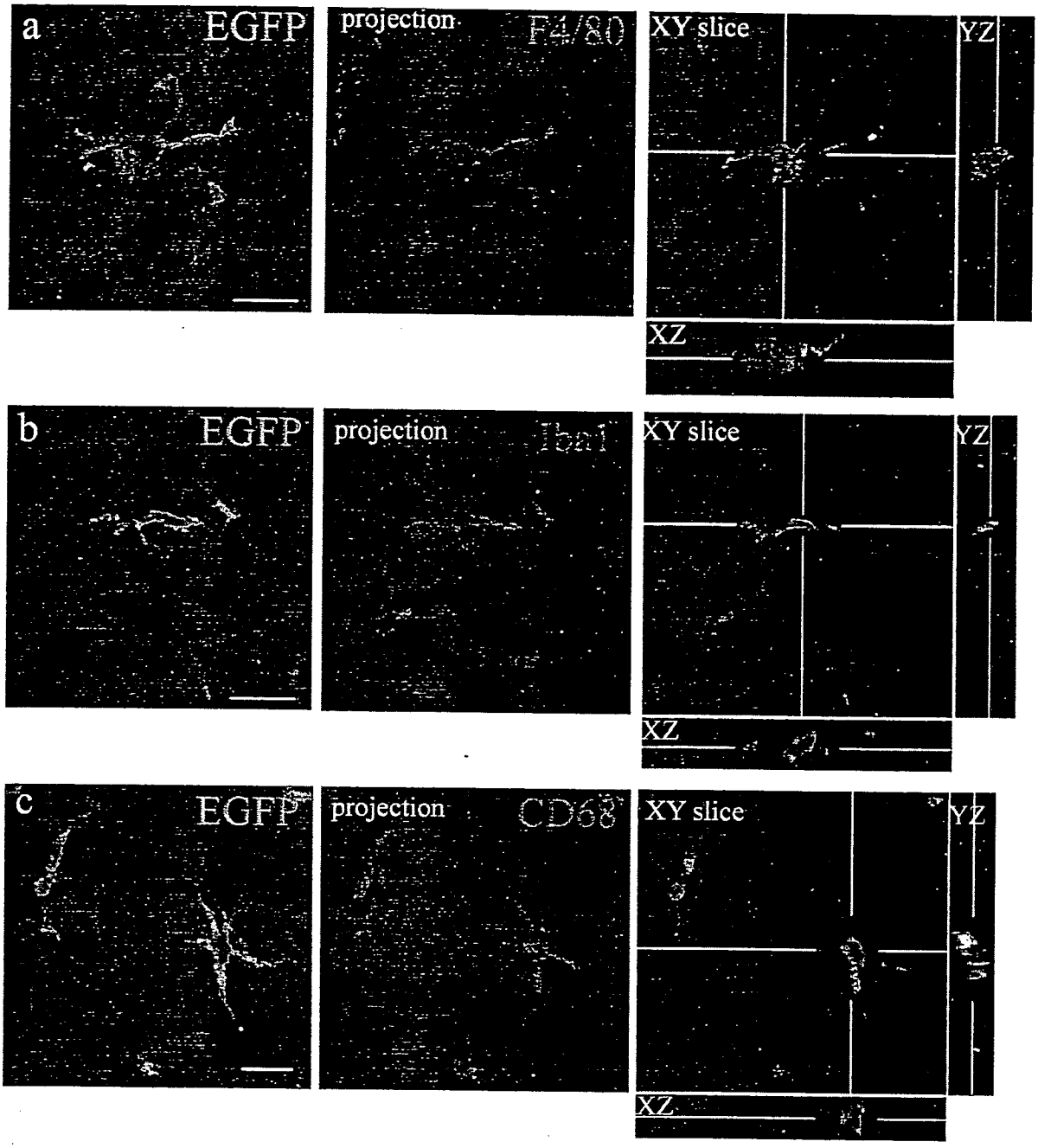

COLOR

Fig. 2. Immunohistochemistry for F4/80, Iba1, and CD68 in the cochleae of bone marrow chimeric mice 6 months after transplantation. **a:** Photomicrographs obtained by confocal microscopy demonstrate colocalization of EGFP and F4/80 in the cells derived from transplanted HSCs within the spiral ganglion (SG). Immunoreactivity for F4/80 was frequently observed in HSC-derived cells in the lower part of spiral ligament (SL) and the SG. **b:** Iba1 expression was also found in HSC-derived cells in the SL and SG. With confocal microscopy, HSC-derived cells in SL are found to be dually labeled with EGFP and Iba1. **c:** CD68 was also colocalized in BM-derived cells expressing Iba1 in SL. Scale bars = 20 μm.

± 5.0% of EGFP-positive cells, and 87.3% ± 2.6% of Iba1-positive cells coexpressed CD68, which also demonstrated that BM-derived cells expressing Iba1 were of macrophage lineage.

Observation of BM-derived cells expressing Iba1 in the cochlea with a confocal microscope revealed a specific morphological feature that was characterized by a spindle shape with several ramified processes, a characteristic morphological feature of macrophages (Fig. 2a–c). In addition to the immunohistochemistry phenotype, BM-derived cells expressing Iba1 in the cochlea morophologically followed microglias that are referred to as resident tissue macrophages in the CNS.

Systemic Application of M-CSF Increased the Number of Iba1-Positive Cells in the Cochlea

To characterize Iba1-positive cells in the cochlea, we next examined the mobilization of Iba1-positive cells using systemic application of M-CSF, the primary regulator of activation of mononuclear phagocytes in wild-type C57BL/6 mice. Iba1-positive cells in both SL and SG were observed more densely in M-CSF-treated mice (Fig. 3a,b) than in controls (Fig. 3c,d). The density of Iba1-positive cells in SL of the middle turn in the controls was 1.46 ± 0.22 (cells/10^4 μm^2), which increased to 2.54 ± 0.45 after M-CSF treatment (Fig. 3e), although the difference was not significant. By contrast, a significant increase was identified in the density of Iba1-positive cells in SG (from 1.39 ± 0.18 to 2.95 ± 0.3; Fig. 3e). These data revealed that Iba1-positive cells in the cochlea are under the control of M-CSF signaling. In addition to the findings of phenotype and morphology, we have demonstrated that BM-derived cells labeled with Iba1 have a quality of resident tissue macrophage in the cochlea.

Cochlear Macrophages Gradually Turn Over for More Than 6 Months

The percentage of chimerism in the peripheral blood at 3 months after BM transplantation was 82.8% ± 3.6%, indicating that hematopoietic reconstitution was performed successfully at this time point. The chimeric ratio observed in the present study was compatible with previous reports on BM chimeric mice (Yoshimoto et al., 2003; Lang et al., 2006). Sequential observation of Iba1-positive cells in the cochlea of transplanted mice demonstrated that cochlear macrophages labeled with Iba1 survived systemic irradiation and were gradually replaced by EGFP-positive cells derived from transplanted HSCs. One or two weeks after HSC transplantation, no EGFP-positive cells were found within cochlear tissues. By contrast, at 4 weeks after transplantation, expression of EGFP was found in 15.4% ± 6.6% of Iba1-positive cells in the cochlea. The ratio for EGFP expression in Iba1-positive cells increased remarkably to 64.9% ± 8.1% in cochlear specimens obtained at 3 months (12 weeks) after transplantation, then reached 84.1% ± 1.6% at 6 months (24 weeks) after transplantation. The differences in the ratio for EGFP expression in Iba1-positive cells were significant at 3 and 6 months compared with 1, 2, or 4 weeks (Fig. 4). The distribution of Iba1-positive cells in the cochlea was identical at each time point (data not shown). The density of Iba1-positive cells in SL was 2.39 ± 0.32 (cells/10^4 μm^2) at

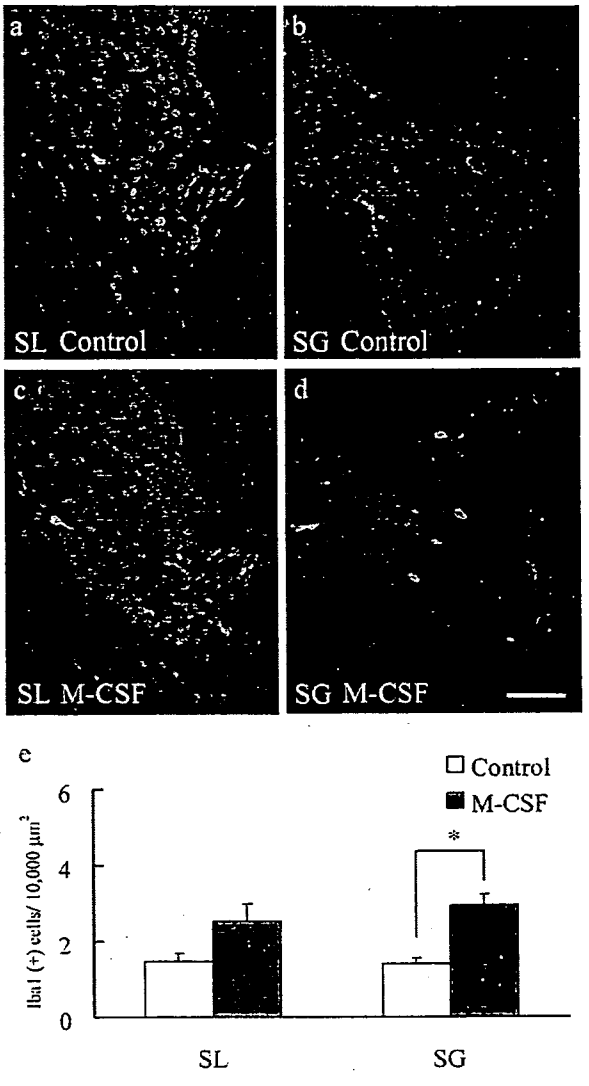

Fig. 3. Systemic application of macrophage colony-stimulating factor increases the density of Iba-1-positive cells in the spiral ligament (SL) and spiral ganglion (SG). **a–d:** Several Iba1-positive cells were found in the SL (c) and the SG (d) following systemic application of macrophage colony-stimulating factor (M-CSF), although few cells expressing Iba1 were observed in control specimens (a,b). **e:** Densities of Iba1-positive cells (cells/10^4 μm^2) in SG of M-CSF-treated cochleae were significantly higher than those of control cochleae (*P = 0.002, unpaired t-test), although no significant difference is found in SL (P = 0.06). Bars represent standard errors. Scale bar = 50 μm.

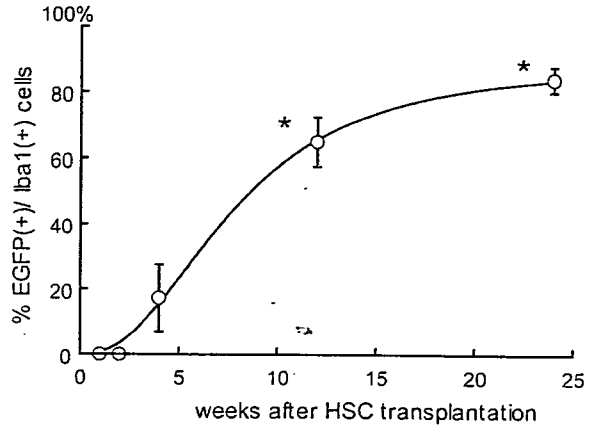

Fig. 4. Sequential analysis of chimeric ratios for Iba1-positive cells following transplantation of hematopoietic stem cells derived from GFP mice. The ratios for EGFP expression in Iba1-positive cells of the whole cochlea are shown at 1, 2, and 4 weeks and 3 (12 weeks) and 6 (24 weeks) months after transplantation. The graph demonstrates a gradual increase in the ratio of EGFP expression in Iba1-positive cells, indicating replacement of native Iba1-positive cells by EGFP-positive cells derived from engrafted hematopoietic stem cells. The ratio at 3 or 6 months is significantly higher than that at 1, 2, or 4 weeks (*$P < 0.001$, ANOVA with Tukey-Kramer's test). Bars show standard errors.

1 week, 2.67 ± 0.07 at 2 weeks, 3.02 ± 0.42 at 4 weeks, 3.25 ± 0.18 at 3 months, and 3.31 ± 0.11 at 6 months after BM transplantation. The density of Iba1-positive cells in SG was 1.35 ± 0.10 (cells/10^4 μm^2) at 1 week, 1.73 ± 0.37 at 2 weeks, 1.22 ± 0.15 at 4 weeks, 1.93 ± 0.32 at 3 months, and 2.26 ± 0.14 at 6 months after BM transplantation. There were no significant differences in the density of Iba1-positive cells in SL among the experimental groups. However, the increase with age in the density of Iba1-positive cells in SG was statistically significant between 1 week and 6 months and between 4 weeks and 6 months. These findings indicate that cochlear macrophages are not eliminated by systemic irradiation and gradually turn over for more than 6 months in nondamaged cochlea.

Cochlear Macrophages Increased in Response to Local Surgical Stress

To examine the reaction of cochlear macrophages to an acute, local, exogenous stress on the cochlea, surgical invasion with application of physiological saline via PSCC was performed on both wild-type and BM chimeric mice. ABR recoding was performed to determine the extent of functional damage following treatment. Significant elevation of ABR thresholds was observed on day 1 after local treatment, whereas no elevation was found on days 7 and 28 at all frequencies (Fig. 5a), indicating that the surgical stress used in the present study caused temporary damage to the cochlea.

Iba1-positive cells were increased temporarily in response to local surgical stress in SL and SG (Fig. 5b–e). The density of Iba1-positive cells in SL exhibited an immediate response to the treatment on day 1 after surgery (3.96 ± 0.16 cells/10^4 μm^2 vs. 1.62 ± 0.18, preoperative), significantly increased on day 7 after surgery (5.42 ± 0.59), and decreased on day 28 (2.90 ± 0.41; Fig. 5f). No significant difference was found in the densities of Iba1-positive cells between before surgery, on day 1, or on day 28. A temporary increase was also found in the density of Iba1-positive cells in SG on day 1 (1.94 ± 0.06) and day 7 (2.66 ± 0.33; Fig. 5f) compared with densities of 1.20 ± 0.09 preoperatively and 1.33 ± 0.16 on day 28. The differences between preoperative values and day 7 and between days 7 and 28 were statistically significant.

We also examined the effect of local surgical stress in BM chimeric mice that had been transplanted with HSCs labeled with EGFP 3 months before, to test the mobilization of Iba1-positive cell from BM to the cochlea. The density of cells dually labeled with EGFP and Iba1 studied in SL at day 7 after treatment was 4.01 ± 0.21 (cells/10^4 μm^2) in the operated group and 2.54 ± 0.39 in nonoperated BM chimeric mice, and that in SG was 1.88 ± 0.52 in the operated group and 1.42 ± 0.21 in the nonoperated group. The difference in the density of EGFP-positive cells in SL between the two groups was statistically significant, whereas that in SG was not significant.

Immunohistochemistry for Ki67 was performed before and at days 1 andf 7 after surgical treatment, to test whether the increase in cochlear macrophages following surgical treatment was due to proliferation in situ. On day 1 following treatment, 1.75 ± 0.85 cells/section were found to be dually labeled with Ki67 and CD68 (1.74 ± 0.71% in total number of cells positive for CD68). On day 7 following treatment, 2.25 ± 0.75 were dually labeled with Ki67 and CD68 (2.49% ± 0.81%), in contrast to 1.00 ± 0.40 in untreated mice (1.53% ± 0.51%). All Ki67-positive cells in the three groups were found in the lower part of SL. However, no statistically significant difference was observed in the number of Ki67-positive cells among the three groups. These findings indicated that the increase in cochlear macrophages was due mainly to the migration of macrophages from the circulation into the cochlea. However, it was also revealed that the proliferation of macrophages in situ is one of the possible sources for cochlear macrophages.

DISCUSSION

The present study revealed that BM-derived cells are supplied continuously to the cochlea even in the adult mouse and demonstrated that the predominant phenotype of macrophages involved expression of CD68, F4/80, or Iba1 in SL and SG. Our study on the morphology, immunohisotochemical phenotype, and reactivity to M-CSF provides evidence that hematopoi-

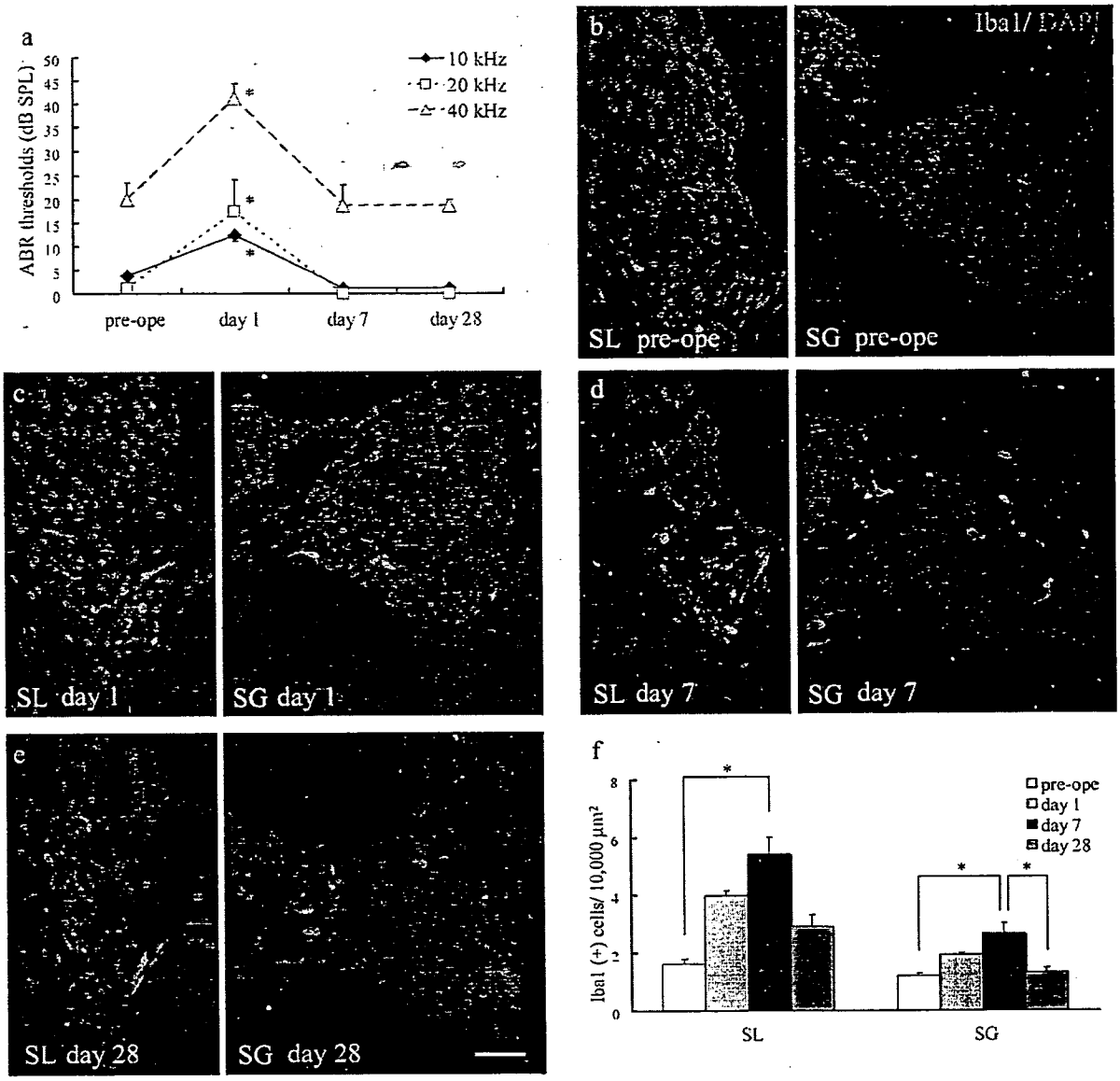

Fig. 5. Effects of local surgical stress on densities of Iba1-positive cells in the spiral ligament (SL) and spiral ganglion (SG). **a:** Local surgical stress causes significant elevation of ABR thresholds at each frequency on day 1 after treatment ($*P < 0.001$, ANOVA with Tukey-Kramer's test), and the elevation recovered on days 7 and 28 at all the frequencies tested. **b–e:** Immunostaining for Iba1 in cochlear specimens obtained preoperatively (pre-ope; b) and on day 1 (c), day 7 (d), and day 28 (e) after treatment. Increase in Iba1-positive cells was observed in the SL and SG of cochleae obtained on days 1 and 7. **f:** The density of Iba1-positive cells (cells/10^4 μm^2) on day 7 was significantly higher than that in preoperative specimens in both SL ($*P = 0.003$) and SG ($*P = 0.002$) or day 28 in SG. Bars show standard errors. Scale bars = 50 μm.

etic BM-derived cells expressing Iba1 are constitutively present as resident tissue macrophages in the cochlea. The examination of the recruitment of cochlear macrophages demonstrated that these cells exhibited slow turnover for several months during steady-state conditions and quickly increased in response to local surgical stress.

Although earlier studies have demonstrated infiltration of inflammatory cells, including macrophages, into the cochlea following inner ear injury (Fredelius, 1988; Bhave et al., 1998; Hirose et al., 2005; Tornabene et al., 2006; Ladrech et al., 2007), two recent studies have suggested the presence of resident tissue macrophages in the inner ear.

Lang et al. (2006) reported that BM-derived cells are constitutively present and widely distributed in the cochlea in the same manner demonstrated in the present study. Although they concluded negatively that only 5% of BM-derived cells differentiated into CD45R-positive macrophages, the rate for CD45 expression in BM-derived cells is also compatible with the present study. The authors instead emphasized that histological analysis of the cochleae following HSCs revealed the contribution of BM-derived cells to fibrocytes or mesenchymal cells in the inner ear. However, the specific ratios for immunoreactivity of Na, K-ATPase, or the Na-K-Cl transporter in the BM-derived cells were not determined in their study. Moreover, there is a discrepancy in the ratio for the expression of F4/80 between the study by Lang et al. (2006) and the present study, although both studies used HSC-transplanted mice that exhibited similar chimeric ratios in peripheral blood and SL cells. One possible explanation for this discrepancy is a difference in methods for immunohistochemistry. We used cryostat sections, whereas Lang et al. used paraffin-embedded sections. Our study demonstrated that more than 80% of BM-derived cells in SL and SG show the phenotype of macrophages and that resident tissue macrophages in the cochlea during steady-state conditions are present in a larger number than reported previously.

Another report was made by Hirose et al. (2005) that CD45-positive mononuclear phagocytes are present in the SL of nonnoise-exposed $CX3CR1^{GFP/GFP}$ transgenic mice, and these cells are also labeled with Iba1 or CD68, which is consistent with the results of the present study. However, the density of CD45-positive cells in the cochlea was quite different between the wild-type and $CX3CR1^{GFP/GFP}$ transgenic mice used in their study, although the number of BM-derived cells expressing CD45 in the cochlea demonstrated in the present study was identical to that of CD45-positive cells in the cochlea of nonnoise-exposed wild-type mice presented by Hirose et al. (2005). The most controversial point is whether it is appropriate to assume that macrophages observed in the cochlea can be described as "microglia-like" cells. Although the authors failed to describe the distribution of macrophages in the auditory nervous system including the SG and cochlear modiolus during steady-state conditions, they distinguish the infiltrating macrophages observed after noise exposure from microglias in the CNS by the morphology and the potentiality of exchanging from the vascular space. The proliferation in situ is thought to be one of the main sources of microglia in adults, but some studies have reported that BM-derived cells can enter the CNS and populate the microglial cell compartment (Lawson et al., 1992; Corti et al., 2002; Hess et al., 2004; Simard and Rivest, 2004; Malm et al., 2005). Moreover, previous studies in the CNS using flow cytometry or immunohistochemistry defined a profile of characterization of microglial cells corresponding to the following phenotype: $CD68^+$, CD45 low, $CD11b^+$, CD11c high, and MHC class II^+ (Guillemin and Brew, 2004; Floden and Combs, 2007). Our results on cochlear resident macrophages "$CD68^+$, $Iba1^+$, and $CD45^-$" were compatible with the immunochemical definition of microglias as reported above. In addition, the cochlear resident macrophages were observed in the auditory nervous system as well as in the connective tissue of SL in the present study. Because there is a considerable heterogeneity in the phenotypes of the macrophage lineage, and because resident tissue macrophages share several antigens with infiltrating macrophages (Guillemin and Brew, 2004), further studies should be carried out to define a profile of characterization on both resident and infiltrating macrophages in the cochlea.

Many studies on resident tissue macrophages in other organs have been performed with BM chimeric mice. In terms of replacement of resident tissue macrophages by BM, donor-derived cells are reported rapidly to populate the liver with Kupffer cells, resident macrophages in the liver, within 3 weeks, and donor Kupffer cells in liver transplants are replaced with similar kinetics (Naito et al., 1997). Microglias in the CNS exhibit longer turnover period than cochlear resident macrophages. At 12 months following HSC transplantation, 40% of microglias have been replaced by hematopoietic cells (Hess et al., 2004; Simard and Rivest, 2004). In contrast, Xu et al. (2007) reported that EGFP-positive BM-derived cells infiltrate normal retina in significant numbers at 8 weeks after BM transplantation and that by 6 months all retinal microglia/macrophges were replaced by BM-derived EGFP-positive cells, the turnover rate of which is very similar to that of the inner ear in the present findings. From the viewpoint of turnover rates, cochlear resident macrophages have characteristics as resident macrophages in the retina.

Although BM chimeric mice are a powerful tool for the analysis of the dynamics of BM-derived cells, there are some limitations. The results of BM chimeric mice are obtained under extraordinary conditions; systemic lethal irradiation and following BM transplantation. It is also technically difficult to set an ideal negative control, with irradiation but without BM transplantation. Moreover, it is difficult to exclude completely the possibility that the results observed in this study are caused by irradiation-induced damage. However, despite these limitations in studies using BM chimeric mice, our results provided some new insights into the origin and distribution of cochlear resident macrophages and the possible supply of cochlear macrophages by replenishment with BM-derived cells.

Recent studies have demonstrated multiple key functions of resident tissue macrophages not only in phagocytosis of foreign bodies or senescent cells but also in the production and secretion of cytokines and the regulation of specific immune responses (Gordon and Taylor, 2005). In the CNS, microglias have both neurotrophic and neurotoxic properties (Kreutzberg, 1996; Moore and Thanos, 1996; Streit, 1996) and play an effector role in both innate and adaptive immune responses, allowing the CNS to respond rapidly and

efficiently to a wide range of pathogens (Olson and Miller, 2004). Although it has not been elucidated whether the infiltrating macrophages play beneficial or harmful roles in the maintenance of auditory function, pharmacological intervention in the infiltration of macrophages may be a possible strategy for treatment of SNHL. In conclusion, the resident cochlear macrophages have potential as a therapeutic target by means of controlling their ability of phagocytosis, migration, or release of cyokines in the pathology of inner ear immune disorders.

ACKNOWLEDGMENTS

The authors thank Dr. Masaru Okabe (Osaka University) for generously providing EGFP transgenic mice and Dr. Junko Okano (Department of Anatomy and Developmental Biology, Graduate School of Medicine, Kyoto University) for critical discussion. We are also very thankful to Dr. Hideaki Ogita, Ms. Yoko Nishiyama, Ms. Rika Sadato, Ms. Akemi Saito, Ms. Keiko Nishio, and Ms. Tomoyo Namura for their excellent technical assistance.

REFERENCES

Bhave SA, Oesterle EC, Coltrera MD. 1998. Macrophage and microglia-like cells in the avian inner ear. J Comp Neurol 398:241–256.

Corti S, Locatelli F, Donadoni C, Strazzer S, Salani S, Del Bo R, Caccialanza M, Bresolin N, Scarlato G, Comi GP. 2002. Neuroectodermal and microglial differentiation of bone marrow cells in the mouse spinal cord and sensory ganglia. J Neurosci Res 70:721–733.

Floden AM, Combs CK. 2007. Microglia repetitively isolated from in vitro mixed glial cultures retain their initial phenotype. J Neurosci Methods 164:218–224.

Fredelius L. 1988. Time sequence of degeneration pattern of the organ of Corti after acoustic overstimulation. A transmission electron microscopy study. Acta Otolaryngol 106:373–385.

Gordon S, Taylor PR. 2005. Monocyte and macrophage heterogeneity. Nat Rev Immunol 5:953–964.

Guillemin GJ, Brew BJ. 2004. Microglia, macrophages, perivascular macrophages, and pericytes: a review of function and identification. J Leukocyte Biol 75:388–397.

Hess DC, Abe T, Hill WD, Studdard AM, Carothers J, Masuya M, Fleming PA, Drake CJ, Ogawa M. 2004. Hematopoietic origin of microglial and perivascular cells in brain. Exp Neurol 186:134–144.

Hirose K, Discolo CM, Keasler JR, Ransohoff R. 2005. Mononuclear phagocytes migrate into the murine cochlea after acoustic trauma. J Comp Neurol 489:180–194.

Iguchi F, Nakagawa T, Tateya I, Kim TS, Endo T, Taniguchi Z, Naito Y, Ito J. 2003. Trophic support of mouse inner ear by neural stem cell transplantation. Neuroreport 14:77–80.

Imai Y, Ibata I, Ito D, Ohsawa K, Kohsaka S. 1996. A novel gene iba1 in the major histocompatibility complex class III region encoding an EF hand protein expressed in a monocytic lineage. Biochem Biophys Res Commun 224:855–862.

Kim TS, Nakagawa T, Kitajiri S, Endo T, Takebayashi S, Iguchi F, Kita T, Tamura T, Ito J. 2005. Disruption and restoration of cell-cell junctions in mouse vestibular epithelia following aminoglycoside treatment. Hear Res 205:201–209.

Kreutzberg GW. 1996. Microglia: a sensor for pathological events in the CNS. Trends Neurosci 19:312–318.

Ladrech S, Wang J, Simonneau L, Puel JL, Lenoir M. 2007. Macrophage contribution to the response of the rat organ of Corti to amikacin. J Neurosci Res 85:1970–1979.

Lang H, Ebihara Y, Schmiedt RA, Minamiguchi H, Zhou D, Smythe N, Liu L, Ogawa M, Schulte BA. 2006. Contribution of bone marrow hematopoietic stem cells to adult mouse inner ear: mesenchymal cells and fibrocytes. J Comp Neurol 496:187–201.

Lawson LJ, Perry VH, Gordon S. 1992. Turnover of resident microglia in the normal adult mouse brain. Neuroscience 48:405–415.

Lee JE, Nakagawa T, Kim TS, Iguchi F, Endo T, Dong Y, Yuki K, Naito Y, Lee SH, Ito J. 2003. A novel model for rapid induction of apoptosis in spiral ganglions of mice. Laryngoscope 113:994–999.

Malm TM, Koistinaho M, Parepalo M, Vatanen T, Ooka A, Karlsson S, Koistinaho J. 2005. Bone-marrow-derived cells contribute to the recruitment of microglial cells in response to beta-amyloid deposition in APP/PS1 double transgenic Alzheimer mice. Neurobiol Dis 18:134–142.

Moore S, Thanos S. 1996. The concept of microglia in relation to central nervous system disease and regeneration. Prog Neurobiol 48:441–460.

Naito M, Hasegawa G, Takahashi K. 1997. Development, differentiation, and maturation of Kupffer cells. Microsc Res Techniq 39:350–364.

Nakagawa T, Kim TS, Murai N, Endo T, Iguchi F, Tateya I, Yamamoto N, Naito Y, Ito J. 2003. A novel technique for inducing local inner ear damage. Hear Res 176:122–127.

Okabe M, Ikawa M, Kominami K, Nakanishi T, Nishimune Y. 1997. 'Green mice' as a source of ubiquitous green cells. FEBS Lett 407:313–319.

Okano T, Nakagawa T, Kita T, Endo T, Ito J. 2006. Cell-gene delivery of brain-derived neurotrophic factor to the mouse inner ear. Mol Ther (in press).

Olson JK, Miller SD. 2004. Microglia initiate central nervous system innate and adaptive immune responses through multiple TLRs. J Immunol 173:3916–3924.

Shiga A, Nakagawa T, Nakayama M, Endo T, Iguchi F, Kim TS, Naito Y, Ito J. 2005. Aging effects on vestibulo-ocular responses in C57BL/6 mice: comparison with alteration in auditory function. Audiol Neurootol 10:97–104.

Shinohara T, Bredberg G, Ulfendahl M, Pyykko I, Olivius NP, Kaksonen R, Lindstrom B, Altschuler R, Miller JM. 2002. Neurotrophic factor intervention restores auditory function in deafened animals. Proc Natl Acad Sci U S A 99:1657–1660.

Simard AR, Rivest S. 2004. Bone marrow stem cells have the ability to populate the entire central nervous system into fully differentiated parenchymal microglia. FASEB J 18:998–1000.

Streit WJ. 1996. The role of microglia in brain injury. Neurotoxicology 17:671–678.

Tornabene SV, Sato K, Pham L, Billings P, Keithley EM. 2006. Immune cell recruitment following acoustic trauma. Hear Res 222:115–124.

Xu H, Chen M, Mayer EJ, Forrester JV, Dick AD. 2007. Turnover of resident retinal microglia in the normal adult mouse. Glia 55:1189–1198.

Yoshimoto M, Shinohara T, Heike T, Shiota M, Kanatsu-Shinohara M, Nakahata T. 2003. Direct visualization of transplanted hematopoietic cell reconstitution in intact mouse organs indicates the presence of a niche. Exp Hematol 31:733–740.